



Published in final edited form as:

Oncogene. 2017 May 25; 36(21): 2981–2990. doi:10.1038/onc.2016.452.

Transamidase site-targeted agents alter the conformation of the transglutaminase cancer stem cell survival protein to reduce GTP binding activity and cancer stem cell survival

Candace Kerr¹, Henryk Szmecinski¹, Matthew L. Fisher¹, Bailey Nance¹, Joseph R. Lakowicz¹, Abdullah Akbar⁶, Jeffrey W. Keillor⁶, Tin Lok Wong⁵, Raquel Godoy-Ruiz⁵, Eric A. Toth^{1,4,5}, David J. Weber^{1,4,5}, and Richard L. Eckert^{1,2,3,4}

¹Department of Biochemistry and Molecular Biology, The University of Maryland School of Medicine, Baltimore, Maryland, 21201 ²Department of Dermatology, The University of Maryland School of Medicine, Baltimore, Maryland, 21201 ³Department of Reproductive Biology, The University of Maryland School of Medicine, Baltimore, Maryland, 21201 ⁴Marlene and Stewart Greenebaum Cancer Center, The University of Maryland School of Medicine, Baltimore, Maryland, 21201 ⁵Institute for Bioscience and Biotechnology Research, and Center for Biomolecular Therapeutics, Rockville, Maryland ⁶Department of Chemistry and Biomolecular Sciences, University of Ottawa, Ottawa, Ontario

Abstract

Type 2 transglutaminase (TG2) is an important cancer stem cell survival protein that exists in open and closed conformations. The major intracellular form is the closed conformation that functions as a GTP-binding GTPase and is required for cancer stem cell survival. However, at a finite rate, TG2 transitions to an open conformation that exposes the transamidase catalytic site involved in protein-protein crosslinking. The activities are mutually exclusive, as the closed conformation has GTP binding/GTPase activity, and the open conformation transamidase activity. We recently showed that GTP binding, but not transamidase activity, is required for TG2-dependent cancer stem cell invasion, migration and tumor formation. However, we were surprised that transamidase site-specific inhibitors reduce cancer stem cell survival. We now show that compounds NC9, VA4 and VA5, which react exclusively at the TG2 transamidase site, inhibit both transamidase and GTP-binding activities. Transamidase activity is inhibited by direct inhibitor binding at the transamidase site, and GTP binding is blocked because inhibitor interaction at the transamidase site locks the protein in the extended/open conformation to disorganize/inactivate the GTP binding/GTPase site. These findings suggest that transamidase site-specific inhibitors can inhibit GTP binding/signaling by driving a conformation change that disorganizes the TG2 GTP binding

Users may view, print, copy, and download text and data-mine the content in such documents, for the purposes of academic research, subject always to the full Conditions of use:http://www.nature.com/authors/editorial_policies/license.html#terms

Correspondence: Richard L. Eckert, Ph.D., Professor and Chair, John F.B. Weaver Endowed Professor, Department of Biochemistry and Molecular Biology, University of Maryland School of Medicine, 108 N. Greene Street, Baltimore, Maryland 21201, Tel: 410-706-3220, Fax: 410-706-8297; reckert@umaryland.edu.

Conflict of Interest

The authors declare no conflict of interest.

to reduce TG2-dependent signaling, and that drugs designed to target this site may be potent anti-cancer agents.

Keywords

Transglutaminase 2; NC9; VA4; VA5; CP4d; cancer; cancer stem cells; squamous cell carcinoma

Introduction

Transglutaminase type 2 (TG2, EC 2.3.2.13) is a multifunctional protein. It catalyzes calcium-dependent formation of covalent crosslinks (transamidation) between the γ -carboxamide group of a peptide bound glutamine and primary amine substrates (21) and also binds and hydrolyzes GTP as a G-protein signal transduction protein (16, 41). These TG2 activities are associated with specific conformational states (5, 6, 24, 46). Closed TG2 functions as a GTP/GDP binding/signaling protein/GTPase that lacks transamidase activity, while open TG2 has crosslinking activity but lacks GTP binding/signaling activity (23, 24, 27, 46, 46, 51). The closed TG2 conformation predominates in the intracellular environment where calcium levels are low (16, 46). If intracellular calcium levels rise, during cell death or in response to extracellular stimuli, calcium binding shifts TG2 to an open/extended crosslinking conformation which exposes the catalytic triad and activates protein-protein crosslinking (transamidase) activity (33). This calcium-dependent change in conformation is associated with loss of GTP/GDP binding and related signaling (23, 24, 27, 46, 51). Consistent with this model, the crosslinking activity of TG2 is allosterically activated by Ca^{2+} and inhibited by GTP, GDP, and GMP (7, 16, 16, 33). Thus, the TG2 GTP-binding folded/closed (signaling) and the open/extended (crosslinking) structures are mutually exclusive.

Tumor cells survive by circumventing normal cell death processes, which is associated with mutation or overexpression of specific oncogenes and silencing of tumor suppressor genes leading to enhanced cell division (25). Recent studies show that cancer stem cells comprise a subpopulation of tumor cells that possess enhanced survival and tumor formation properties (10, 13, 15). These cells display enhanced invasion, migration and ability to form highly vascularized and rapidly growing tumors as compared to non-stem cancer cells (2, 18, 19). Given the recognition that cancer stem cells are an extremely dangerous tumor subpopulation, an important goal is identification of cancer stem cell survival proteins that are elevated in level or activity in cancer stem cells to serve as therapy targets. Recent studies indicate that TG2 is a cancer stem cell survival protein (15, 18, 19) and suggest that the TG2 GTP binding activity is required and responsible for its function as a survival protein (15). We have shown that intracellular TG2 exists in the closed GTP-binding/G-protein signaling conformation that drives cancer and cancer stem cell survival, invasion, migration and tumor formation (15, 19). The important role of closed conformation TG2 has also been observed in other cancer models (15, 19, 26, 35, 36).

A variety of small molecular inhibitors have been described that target TG2 (22, 29, 32, 47, 50, 55). Most of these are irreversible inhibitors designed to covalently interact with the TG2

catalytic triad of the transamidase site to inhibit transamidase (crosslinking) activity (29). Although these agents inhibit TG2 transamidase activity, less is known about their impact on TG2 conformation or GTP-binding/signaling activity. In the sole study to address the impact of such an agent on intracellular TG2 structure, Truant and associates used a novel fluorescence method to show that NC9 (31), an irreversible inhibitor of TG2 transamidase activity (29, 31), converts intracellular TG2 from a closed to open conformation (11). However, it is not known if this is a generalized phenomenon and if this agent also influences TG2 GTP-binding/G-protein signaling activity.

We have shown that epidermal cancer stem cells (ECS cells) require TG2 GTP binding activity, but not transamidase activity, for cancer stem cell survival (18, 19). Although they are not designed to inhibit TG2 GTP binding, we surprisingly observed that transamidase site-specific inhibitors reduce ECS cell survival and tumor formation (18, 19). To explain this paradox, we propose that covalent transamidation site-specific inhibitors suppress TG2 transamidation (crosslinking) activity and also lock TG2 into the extended (open) conformation, which disorganizes/inactivates the GTP binding site. To test this hypothesis, we examine the impact of irreversible (NC9, VA4, VA5) and reversible (CP4d) TG2 transamidase site-specific inhibitors on TG2 transamidase activity, TG2 structure, and TG2 GTP binding activity. Our findings suggest that although these agents specifically interact with the transamidase catalytic center, they produce a conformational change that results in disorganization/inactivation of the TG2 GTP binding site, leading to reduced cancer stem cell survival.

Results

Transglutaminase 2 level is markedly elevated in cancer stem cells where it functions as a survival factor that is required for efficient cancer stem cell spheroid formation, invasion, migration and tumor formation (15, 18, 19). A role for TG2 in cancer stem cell survival, and in other diseases (16, 40), has driven efforts to develop TG2 inhibitors as therapeutic agents. A number of compounds have been identified that inhibit TG2 transamidase (crosslinking) activity by interacting at the transamidase catalytic site (29). However, cancer stem cell survival requires the GTP binding/G-protein signaling activity of TG2 (15, 16, 18, 19) and it is not known whether transamidase inhibitors may also indirectly inhibit TG2 GTP binding. A finding that agents designed to bind the transamidase site also inhibit TG2 GTP binding would be important, as TG2 inhibitors can be synthesized that specifically bind to the transamidase site but it is more difficult to design agents that target the GTP binding site. We propose that these agents, although they interact with the transamidase catalytic center, produce a conformational change that results in indirect inhibition of TG2 GTP binding to inhibit GTP-dependent TG2 survival signaling (15, 18, 19).

To test this hypothesis we studied the impact of irreversible (NC9, VA4, VA5) and reversible (CP4d) TG2 transamidase site-specific inhibitors on TG2 structure, transamidase activity, and GTP binding (Fig. 1A). We monitored the impact of each inhibitor on intracellular TG2 structure using FLIM (Fluorescence Lifetime Imaging Microscopy). FLIM is a quantitative method of assessing fluorescence lifetime that measures energy transfer between donor and accept probes (12, 37, 38, 48, 54, 54). Fluorescence lifetime is measured in nanoseconds and

a short lifetime correlates with close juxtaposition of the probes (Fig. 1B) (12). An advantage of this method is that fluorescent lifetimes are independent of probe concentration (12). In the present experiments, we express in cells a TG2 fusion protein in which the donor probe (mCER) is fused to the N-terminus and the acceptor probe (YFP) at the C-terminus (11) (Fig. 1B). mCER and YFP comprise an ideal donor/acceptor pair for intracellular FRET studies (11, 49). The donor probe is excited by laser illumination and energy transfer to the acceptor is monitored by measuring donor lifetime. The fluorescent lifetime is shorter when TG2 is in the closed conformation, in which the terminal mCER and YFP are brought close together. SCC-13 cells were electroporated with empty vector, mCER-TG2 or mCER-TG2-YFP. The anti-TG2 protein blot shown in Fig. 1C confirms that each TG2 fusion protein is expressed, and Fig. 1D reveals that the subcellular distribution (cytoplasmic, nuclear and membrane) of each protein mimics that of endogenous TG2 (16).

We first tested the constructs to assure that they respond in the expected manner (11). SCC-13 cells were electroporated with mCer-TG2 or mCer-TG2-YAP and after 24 h incubated with 0 (control) or 10 μ M A23187 for 24 h. A23187, a calcium ionophore, causes an increase in intracellular calcium concentration, which in turn causes TG2 to shift to the extended conformation (46, 51). The cell images in Fig. 1E display the signal intensity and lifetime fluorescence values. The blue and green graphs show the lifetime distribution for control and 10 μ M A23187-treated mCer-TG2-YFP expressing cells. These plots reveal that calcium ionophore (A23187) treatment causes the lifetime to increase from 2.9 to nearly 3.1 ns. The maximal lifetime, determined using the mCer-TG2 construct (absence of YFP acceptor) is 3.15 ns (orange distribution) (Fig. 1E). An identical lifetime for the mCer-TG2 protein was observed in untreated cells (not shown), indicating the calcium treatment does not impact the donor probe non-specifically. The bar graph (Fig. 1E) quantifies the findings from multiple experiments. These plots show that lifetime is markedly increased when mCer-TG2-YFP expressing cells are treated with A23187, indicating that calcium treatment causes TG2 to adopt an open conformation.

Impact of inhibitors on TG2 conformation

We next examined the impact of inhibitors that covalently bind to the TG2 transamidation site. These compounds covalently and irreversibly attach to Cys-277 in the transamidase site catalytic triad, which includes Cys-277, His-335 and Asp-358 (29, 30). Cells expressing mCer-TG2-YFP were treated with increasing concentrations of each compound. Fig. 2 shows that the lifetime is markedly increased in mCer-TG2-YFP expressing cells treated with NC9, VA4 or VA5, showing that these lock TG2 in its open conformation. We also monitored the impact of CP4d, a reversible TG2 inhibitor that competes with the acyl donor substrate for binding at the transamidase site (29, 44). Cells expressing mCer-TG2 or mCer-TG2-YFP were treated with increasing concentrations of CP4d. We found a consistent, but not significant, decrease in fluorescent lifetime following treatment with CP4d (Fig. 3A), indicating that CP4d causes a slight reduction in lifetime suggesting that CP4d either does not influence or slightly closes TG2 structure which is consistent with previous findings (11). As expected, these agents did not alter the lifetime of mCer-TG2 (orange distributions) (Fig. 2 and Fig. 3A).

Inhibitor impact on TG2 GTP binding/signaling activity

The above findings show that NC9, VA4, VA5 and CP4d alter TG2 conformation. We next examined the impact of these agents on TG2 functional activity. We first assessed the impact on transamidation (crosslinking) activity. Cells were preloaded with fluorescein cadaverine (FC), a fluorescein-labeled TG2 transamidase site substrate (28, 42), and then treated with 0 or 20 μM NC9, VA4, VA5 or CP4d (Fig. 1A) for 30 min, followed by treatment with A23187, a calcium ionophore, for 90 min. In this assay, compounds that inhibit TG2 transamidation activity reduce calcium-activated TG2 crosslinking of FC, resulting in reduced cell-retained fluorescence (52, 53). The control cells appear green due to transglutaminase-catalyzed covalent crosslinking of FC to cellular proteins, and this incorporation is drastically reduced in inhibitor-treated cells (Fig. 3B), confirming that these agents inhibit TG2 transamidase activity.

We previously reported that TG2 GTP binding is essential for TG2 promotion of cancer stem cell survival (15, 18, 19). We therefore next assessed whether these transamidase site inhibitors alter TG2 GTP binding. Cells were incubated with 0 or 5 μM of each inhibitor for 24 h. Extracts were then prepared and TG2 binding to GTP-agarose beads was measured by immunoblot (23, 24). The lanes contain identical cell equivalents of extract so that the TG2 GTP-bound fraction can be compared to the total amount of TG2 (Fig. 3C). These studies indicate that essentially all TG2 is in a GTP-bound state in non-treated cells, and that inhibitor treatment reduces the quantity to near-zero. This demonstrates that these inhibitors greatly reduce TG2 GTP-binding activity.

Inhibitors regulate the conformation of recombinant TG2

The studies shown in Figs. 2 and 3 indicate that NC9, VA4 and VA5 shift TG2 to an open conformation in cells. However, it could be argued that this is an indirect effect. To confirm that these agents directly interact with TG2, we examined their effect on purified recombinant TG2. TG2 conformation can be measured by capillary electrophoresis (14) or by native gel electrophoresis (43). In the latter, closed-conformation TG2 migrates more rapidly than the extended form (5, 11, 23, 24, 32, 46). We pre-incubated recombinant TG2 for 1 h with inhibitor and then incubated for an additional hour following addition of 1 mM MgCl_2 and 0 or 500 μM GTP. The samples were then electrophoresed on native gels to measure TG2 conformation. Fig. 3D shows that purified recombinant TG2 is largely in the extended conformation (lane 1) and that GTP addition shifts some to the closed state (Lane 2). Lanes 3 through 8 indicate that pre-incubation with NC9, VA4 or VA5 shifts TG2 from the closed to extended conformation and that this is not reversed by GTP addition. Lanes 9 and 10 indicate that CP4d is less able to shift TG2 to an extended conformation (Fig. 3D). We next examined the impact of simultaneous incubation with inhibitor and 500 μM GTP on inhibitor ability to shift TG2 to the extended conformation. These studies (Fig. 3E) show that the inhibitors do not produce a shift to open form under these conditions, arguing that the presence of GTP maintains the protein in the closed state and prevents inhibitor access to the transamidase site.

TG2 inhibitor biologically activity

Epidermal cancer stem cells (ECS cells) display a specific malignant phenotype that includes spheroid forming capacity, and enhanced invasion and migration (2). Moreover, TG2 has a major role in maintaining and enhancing this phenotype, a role that requires functional GTP binding (15, 18, 19). We therefore tested the effect of each inhibitor on ECS cell biology. Fig. 3F/G shows that NC9, VA4, VA5 and CP4d inhibit spheroid formation (a measure of cancer stem cell survival) (2) and matrigel invasion (a measure of invasive potential) (2) and Fig. 3H shows that these agents inhibit cell migration, leading to reduced closure of a scratch wound (a measure of migration potential).

Inhibitor impact on TG2 structure/activity in HaCaT cells

To determine whether these agents act in a similar manner in other epidermis-derived cell lines, we studied their impact on TG2 structure, TG2 transamidase and GTP binding activity, and ability to suppress survival of ECS cells derived from the HaCaT cell line. HaCaT cells are an immortalized, but not malignant, human epidermal cell line (8). To examine inhibitor impact on TG2 structure, HaCaT cells were electroporated with mCer-TG2 or mCer-TG2-YAP and then treated with inhibitor. Fig. 4A shows that treatment with NC9, VA4 or VA5 increases fluorescence lifetime, indicating that inhibitor treatment shifts TG2 from the closed to the extended conformation. In contrast, and as noted in SCC-13 cells, CP4d produces a minimal change in TG2 structure. We next examined inhibitor impact on TG2 transamidase and GTP binding activity. We show that NC9, VA4, VA5 and CP4d suppress TG2 transamidase activity (as measured by suppression of FC incorporation) (Fig. 4B) and also reduce TG2 GTP binding (Fig. 4C). We next examined the effect of each compound on biological endpoints. Figs. 4D and E show that NC9, VA4, VA5 and CP4d suppress ECS cell spheroid formation and invasion through matrigel, indicating that these agents reduce ECS cell survival and invasive potential.

TG2-null cells are not impacted by NC9

To confirm that TG2 mediates NC9 action, we compared the ability of NC9 to suppress matrigel invasion in ECS cells, derived from SCC-13 cells, engineered to express varying levels of TG2. These include SCC13-Control-shRNA (wild-type levels), SCC13-TG2-shRNA2 (TG2 partial knockdown) and SCC13-TG2-KOc12 (TG2-null) cells (Fig. 4F). The immunoblot shows the level of TG2 in each cell line and confirms the absence of TG2 in SCC13-TG2-KOc12 cells. Invasion is a property of ECS cells that is associated with the transformed state (2, 18, 19). We therefore monitored the ability of 0 or 20 μ M NC9 to suppress invasion in these cells. **Fig. G/H** shows that invasion varies directly with TG2 level, and that NC9 suppression of invasion is inversely related to TG2 level. Moreover, TG2 is clearly required for NC9 suppression of cell invasion, as TG2-null cell invasion is not suppressed by NC9.

Impact of inhibitors on TG2 structure

To understand the molecular changes that occur at the TG2 GTP binding site during inhibitor-induced favoring of the open over the closed conformation, we performed in silico structure analysis based on available structures for the open and closed forms (RCSB

numbers 1KV3 and 2Q3Z, respectively) (39, 46). Fig. 4I shows that the α - and β -phosphates of GDP hydrogen bond with residues R476, R478 and R580 of closed-conformation TG2, and that the guanine base of GDP is cradled in a hydrophobic pocket bracketed by the TG2 M483 and F174 residues. Binding is further stabilized by a hydrogen bond between the O γ of S482 and the guanine exocyclic amino group. When TG2 is in the extended conformation, the hydrogen bonding network that recognizes the α - and β -phosphates of GDP is altered such that R476 and R478 are no longer in position to contact the GDP β -phosphate. Moreover, the hydrophobic pocket is no longer intact because the first β -barrel domain has moved away from the catalytic core, and M483 has shifted such that it clashes, sterically, with N1, C6, and O6 of the guanine base.

Discussion

Recent studies show that TG2 is overexpressed in cancer and is associated with an aggressive cancer phenotype and drug resistance (16). Moreover, TG2 level is highly elevated in cancer stem cells derived from epidermal squamous cell carcinoma (2, 19), breast (3, 34–36), glioma (20) and ovarian (9) cancer, and is required for cancer stem cell survival, migration and invasion (15). We have proposed from existing data and our own experiments, that TG2 must assume a closed (GTP-binding, signaling) conformation (Fig. 1B) to confer cancer cell survival, since mutation of the TG2 GTP binding site results in loss of pro-survival activity (16, 18, 19). These observations suggest that drugs designed to target the TG2 GTP binding site may be useful therapeutic agents. However, the GTP binding domain has proved difficult to selectively target because it shares structural properties with similar sites on other proteins. In contrast, because of its unique structural features, the TG2 transamidation site has been successfully targeted (4, 22, 31, 50). Irreversible inhibitors (NC9, VA4 and VA5) specifically react with Cys-277 in the TG2 transamidation site (31), and CP4d competitively suppresses substrate access to the transamidation site (32).

The sites responsible for transamidase activity and GTP binding are located at spatially distinct locations on the protein and so it was anticipated that transamidase inhibitor interaction with TG2 would not inhibit GTP binding. However, we were surprised to observe that NC9, a transamidase site-specific inhibitor, suppresses epidermal cancer stem cell survival (18, 19). Since TG2-dependent stimulation of cancer stem cell survival requires GTP binding activity (19), this finding suggests that the transamidase site-specific inhibitor may alter GTP binding. In the present study we test the hypothesis that inhibitor interaction at the TG2 transamidase site confers a conformation change in TG2 and thereby disorders the GTP binding site to reduce GTP binding. We use a novel fluorescence lifetime method (11, 45) to measure the conformation of TG2 in intact cells. This method involves monitoring the distance between fluorescent probes fused at the amino (mC_{er}) and carboxyl (YAP) termini of TG2 (11, 45). Our results show that binding of irreversible inhibitors (NC9, VA4, VA5) at the transamidase catalytic site cysteine (Cys-277) favors a shift in the conformational equilibrium of intracellular TG2 from a closed to open conformation, while suppressing GTP binding. These agents also suppress ECS cell survival, invasion and migration. These results suggest that covalent interaction of the irreversible inhibitors at the transamidase site locks TG2 in an extended/open conformation, which disorders the GTP binding site, reducing GTP binding and leading to suppression of TG2 pro-survival activity.

Although the acyl-donor substrate competitive inhibitor CP4d has a minimal impact on TG2 conformation, it also suppresses TG2 GTP binding and suppresses ECS cell survival. We interpret this to mean that while the competitive inhibitor may also produce a TG2 conformation change, this change is not readily detected in our assay system because CP4d does not irreversibly interact with site Cys-277, which permits TG2 to continue to undergo open/closed conformation state changes.

It could be suggested that these inhibitors act via an indirect mechanism to modulate TG2 function. We proposed that these agents target TG2 in ECS cells for several reasons. First, TG2 localizes predominantly in the cytoplasm and the fact that these compounds alter TG2 conformation and activity, suggests they have access to the cell interior. Second, it could be argued that these agents act by impacting unknown proteins. The major candidate targets would be other transglutaminases, including FXIIIa and TG1, which are expressed at low levels in ECS cells (19). This appears very unlikely, because of the low levels of FXIIIa and TG1 in these cells and because we have shown they do not have a biological role in mediating ECS cell survival (19). Moreover, these compounds are not active in TG2 knockout ECS (Fig. 4F/G/H), suggesting that they do not act via alternate/non-specific targets. Third, we show that TG2 directly alters the structure of recombinant TG2. In this context, we show that pre-incubation of recombinant TG2 with NC9, VA4 or VA5 shifts TG2 to the open state and that this shift is not reversed by subsequent addition of GTP. In contrast, simultaneous addition of inhibitor and GTP does not result in an inhibitor-dependent shift of TG2 to the open/extended conformation. These studies suggest that the inhibitors directly interact with TG2 to promote the conformation change, and that the presence of GTP maintains recombinant TG2 in the closed state and impedes inhibitor access to the transamidase site. Taken together, these findings make a strong case that these agents selectively and directly target TG2 to reduce ECS cell survival.

Since most of the residues that comprise the GTP/GDP-binding pocket in closed TG2 reside in the TG2 first β -barrel domain, it is instructive to examine whether this domain remains competent to bind GTP/GDP in the TG2 open conformation. We therefore attempted to dock GDP to a model of the TG2 open conformation. This analysis shows that in open/extended TG2, the TG2 residues that engage in hydrogen bonding with GDP are oriented such that they do not appropriately contact GDP. The most severe perturbations occur in the hydrophobic pocket that envelops the guanine base. In closed conformation TG2, M483 and F174 form the face of this pocket. The position of M483 is stabilized by interactions with L584 and E585, which are in turn buttressed by interactions with K176. Similarly, F174 engages in aromatic stacking with the guanine base that is in part stabilized by van der Waals interactions with Y583. In contrast, two major changes occur in the guanine-binding pocket in the TG2 open form. First, the conformational shift that opens TG2 moves F174 approximately 45 Å from the guanine-binding pocket. Second, M483 shifts such that it sterically clashes with the GDP guanine base. These changes result in reduced GDP binding capacity of extended conformation TG2.

Based on these findings, we propose that inhibitors that specifically bind to the TG2 transamidase site can shift the conformational equilibrium of TG2 to favor the open conformation and that this conformation change disorganizes the GTP binding site to reduce

GTP binding and GTP-related TG2 signaling. The ultimate impact is to reduce cancer stem cell survival, invasion and migration. Thus, these studies suggest that TG2 transamidation site inhibitors that impact the conformational equilibrium deserve attention and development as potential anti-tumor agents. Indeed, studies to be published elsewhere show that NC9 suppresses the ability of SCC-13 cell-derived ECS cells to form tumors in a subcutaneous xenograft model.

Materials and Methods

Antibodies and reagents

Dulbecco's modified Eagle's medium (11960-077), sodium pyruvate (11360-070), L-Glutamine (25030-164), and 0.25% trypsin-EDTA (25200-056) were from Gibco. Heat-inactivated FCS (F4135), anti- β -actin (A5441), A23187 ionophore was from Sigma (C7522). Anti-green fluorescent protein was from Abcam (ab290). Cell lysis buffer (9803) was from Cell Signaling Technology. Anti-TG2 (MAB3839) was from EMD Millipore. Synthesis of the NC9, and CP4d TG2 inhibitors is described elsewhere (31, 44). VA4 and VA5 were synthesized by Akbar and Keillor (unpublished). Fluorescein cadaverine (FC) was from Life Technologies. BD Biocoat cell inserts (353097) and Matrigel (354234) were from BD Biosciences. Measurement of significant difference was performed using the student's T test with a minimum of three independent repeated experiments.

Electroporation

Plasmids encoding mCer-TG2 or mCer-TG2-YFP(linker), referred to in the present paper as mCer-TG2-YFP, cloned in EC1214 vector were provided by Dr. Ray Truant (McMaster University, Ontario, Canada) (11). Cells were electroporated using the Amaxa electroporator and the VPD-1002 nucleofection kit (Amaxa, Cologne, Germany). Cells were harvested with trypsin and replated one day before use. On electroporation day, one million cells were harvested with trypsin, washed with 1 ml of sterile phosphate-buffered saline (pH 7.5), and suspended in 100 μ l of nucleofection solution. The cell suspension, including 3 μ g of plasmid, was gently mixed and electroporated using the T-018 settings. Warm medium (500 μ l) was added and the suspension was transferred to a 60 mm cell culture plate containing 1.5 ml of medium.

In situ TG2 transamidase activity assay

Cells (40,000) were plated in 24-well attachment dishes in spheroid media and grown until 50% confluent. Fluorescein cadaverine (FC) was added in 2 ml of serum-free medium at a final concentration of 20 μ M and incubated for 4 h. The wells were washed twice with serum-free spheroid medium, and then 2 ml of fresh serum-free medium was added containing vehicle (DMSO) or 20 μ M of NC9, VA4, VA5 or CP4d. After 30 min, the wells were supplemented with 10 μ M A23187, a calcium ionophore, with permits calcium influx leading to activation of TG2 transamidase activity. Cells were incubated for an additional 90 min and then washed three times with $\text{Ca}^{++}/\text{Mg}^{++}$ -free HBSS, fixed with formalin, washed with PBS, and imaged to detect covalent FC incorporation (17, 28).

Fluorescence lifetime imaging

Fluorescence lifetime images were acquired using a FLIM system (Alba 5 from ISS). The excitation was from a pulsed laser diode 443 nm coupled with a scanning mirrors module (ISS) through a 443/532/635 nm multiband dichroic filter (Semrock) to a microscope (Olympus IX71S) equipped with a 20× 0.45 NA objective (UPlan Olympus). Emission was observed through bandpass filter 480/35 nm (Chroma Technology) and detected by a photomultiplier H7422-40 (Hamamatsu). FLIM data were acquired using a time-domain modality (SPC-830 TCSPC module from Becker and Hickl GmbH). Images were acquired using an image size of 256 × 256 pixels and a pixel dwell time of 1 ms. To account for intensity heterogeneity within single intensity images, two to five consecutive scans were acquired and summed to build FLIM intensity images for lifetime analysis. Image frame sizes were varied to accommodate multiple cells expressing mCer-TG2 or mCer-TG2-YFP (11) (from about 400 × 400 μm² to about 100 × 100 μm²). FLIM data were analyzed using VistaVision Suite software (Vista v.213 from ISS). Lifetime images were generated by fitting data using a single exponential intensity decay model. The intensity threshold for lifetime analysis was set at least 3-fold above the intensity of dim cells and the fitting procedure was performed for binned pixels at a level of 3 (7 × 7 pixels). Lifetime distribution within an image is represented by a histogram showing pixel frequency at a specific lifetime. The average lifetime values with standard deviations were calculated based on all processed pixels in a lifetime image. FRET values were calculated according to the formula $ET = 1 - (T_{DA} / T_D)$, where T_D is the lifetime of the donor fluorophore (mCer-TG2) and T_{DA} is the lifetime of donor-acceptor pair (mCer-TG2-YFP).

TG2 GTP binding assay

The GTP binding/GTP-agarose pull-down assay was as described (23, 24). Cells were incubated for 24 h in spheroid media containing 0 or 5 μM VA4, VA5, NC9 or CP4d. After trypsinization, the cells were rinsed in ice-cold PBS, pelleted, and resuspended in GTP-binding buffer containing 20 mM Tris-HCl pH = 7.5, 5 mM MgCl₂, 2 mM PMSF, 20 μg/ml leupeptin, 20 μg/ml pepstatin, 10 μg/ml aprotinin plus 150 mM NaCl and 0.1% Triton-X. The cells were sonicated for 15 s, centrifuged at 13,000 g for 10 min at 4°C, and the supernatant was collected. A fraction of the supernatant was set aside for electrophoresis to determine total TG2 level. Supernatant protein (100 μg) was incubated with 100 μl of GTP-agarose beads (Sigma-Aldrich, pre-equilibrated in GTP-binding buffer), in a total of 500 μl of GTP-binding buffer for 30 min at 4°C. The beads were centrifuged at 10,000 g for 2 min and the supernatant retained. The beads were then again washed three times with 1 ml of GTP-binding buffer and the retained supernatant was incubated with the beads for another 30 min. The beads were washed and incubated with the retained supernatant overnight at 4°C. The beads were then washed seven times with GTP-binding buffer, and bound protein was eluted by boiling in 100 μl of 2 × Laemmli buffer. The samples (50 μg protein equivalents, 50 μl) were then electrophoresed for anti-TG2 immunoblot. Total supernatant (50 μg protein) was electrophoresed in parallel.

Inhibitor modulation of recombinant TG2 conformation

Recombinant TG2 protein was prepared as described (39) with the exception that neither GTP nor ATP were included in the lysis buffer. TG2 protein (3.3 μ M, 8 μ g per 30 μ l reaction) was pre-incubated with 0 or 500 μ M NC9, VA4, VA5 or CP4d for 1 h in 75 mM imidazole, 0.5 mM EDTA, 5 mM DTT, pH 7.2 prior to addition of 500 μ M GTP/1 mM $MgCl_2$ and further incubation for 1 h at 25 $^{\circ}C$ (46). In some experiments, inhibitor and GTP were added simultaneously. Laemmli native loading buffer was added, and 6 μ g of protein was electrophoresed on a native 4% to 6% acrylamide gel and electrophoresed at 125 V for 45 min at 4 $^{\circ}C$ using Tris-glycine buffer (5, 46). The gel was fixed in 40% methanol/10% acetic acid for 30 min, stained with 0.25% Coomassie R-250, destained overnight with 10% methanol/10% acetic acid and photographed.

Spheroid formation, invasion and migration assays

Spheroid formation, invasion and migration assays were performed as in our previous reports (1, 2, 18).

Acknowledgments

This work was supported by National Institutes of Health grants R01-CA184027 and R01-CA131074 to Richard Eckert.

References

1. Adhikary G, Grun D, Balasubramanian S, Kerr C, Huang J, Eckert R. Survival of skin cancer stem cells requires the Ezh2 polycomb group protein. *Carcinogenesis*. 2015 **in press**.
2. Adhikary G, Grun D, Kerr C, Balasubramanian S, Rorke EA, Vemuri M, et al. Identification of a population of epidermal squamous cell carcinoma cells with enhanced potential for tumor formation. *PLoS One*. 2013; 8:e84324. [PubMed: 24376802]
3. Agnihotri N, Kumar S, Mehta K. Tissue transglutaminase as a central mediator in inflammation-induced progression of breast cancer. *Breast Cancer Res*. 2013; 15:202. [PubMed: 23673317]
4. Badarau E, Collighan RJ, Griffin M. Recent advances in the development of tissue transglutaminase (TG2) inhibitors. *Amino Acids*. 2013; 44:119–127. [PubMed: 22160259]
5. Begg GE, Carrington L, Stokes PH, Matthews JM, Wouters MA, Husain A, et al. Mechanism of allosteric regulation of transglutaminase 2 by GTP. *Proc Natl Acad Sci U S A*. 2006; 103:19683–19688. [PubMed: 17179049]
6. Begg GE, Holman SR, Stokes PH, Matthews JM, Graham RM, Iismaa SE. Mutation of a critical arginine in the GTP-binding site of transglutaminase 2 disinhibits intracellular cross-linking activity. *J Biol Chem*. 2006; 281:12603–12609. [PubMed: 16522628]
7. Bergamini CM. GTP modulates calcium binding and cation-induced conformational changes in erythrocyte transglutaminase. *FEBS Lett*. 1988; 239:255–258. [PubMed: 2903073]
8. Boukamp P, Petrussevska RT, Breitkreutz D, Hornung J, Markham A, Fusenig NE. Normal keratinization in a spontaneously immortalized aneuploid human keratinocyte cell line. *J Cell Biol*. 1988; 106:761–771. [PubMed: 2450098]
9. Cao L, Shao M, Schilder J, Guise T, Mohammad KS, Matei D. Tissue transglutaminase links TGF-beta, epithelial to mesenchymal transition and a stem cell phenotype in ovarian cancer. *Oncogene*. 2012; 31:2521–2534. [PubMed: 21963846]
10. Cariati M, Purushotham AD. Stem cells and breast cancer. *Histopathology*. 2008; 52:99–107. [PubMed: 18171421]
11. Caron NS, Munsie LN, Keillor JW, Truant R. Using FLIM-FRET to measure conformational changes of transglutaminase type 2 in live cells. *PLoS One*. 2012; 7:e44159. [PubMed: 22952912]

12. Chen Y, Mills JD, Periasamy A. Protein localization in living cells and tissues using FRET and FLIM. *Differentiation*. 2003; 71:528–541. [PubMed: 14686950]
13. Clevers H. The cancer stem cell: premises, promises and challenges. *Nat Med*. 2011; 17:313–319. [PubMed: 21386835]
14. Clouthier CM, Mironov GG, Okhonin V, Berezovski MV, Keillor JW. Real-time monitoring of protein conformational dynamics in solution using kinetic capillary electrophoresis. *Angew Chem Int Ed Engl*. 2012; 51:12464–12468. [PubMed: 23132828]
15. Eckert RL, Fisher ML, Grun D, Adhikary G, Xu W, Kerr C. Transglutaminase is a tumor cell and cancer stem cell survival factor. *Mol Carcinog*. 2015; 54:947–958. [PubMed: 26258961]
16. Eckert RL, Kaartinen MT, Nurminskaya M, Belkin AM, Colak G, Johnson GV, et al. Transglutaminase regulation of cell function. *Physiol Rev*. 2014; 94:383–417. [PubMed: 24692352]
17. Eckert RL, Sturniolo MT, Jans R, Kraft CA, Jiang H, Rorke EA. TIG3: a regulator of type I transglutaminase activity in epidermis. *Amino Acids*. 2009; 36:739–746. [PubMed: 18612777]
18. Fisher ML, Adhikary G, Xu W, Kerr C, Keillor JW, Eckert RL. Type II transglutaminase stimulates epidermal cancer stem cell epithelial-mesenchymal transition. *Oncotarget*. 2015; 6:20525–20539. [PubMed: 25971211]
19. Fisher ML, Keillor JW, Xu W, Eckert RL, Kerr C. Transglutaminase is required for epidermal squamous cell carcinoma stem cell survival. *Mol Cancer Res*. 2015; 13:1083–1094. [PubMed: 25934691]
20. Fu J, Yang QY, Sai K, Chen FR, Pang JC, Ng HK, et al. TGM2 inhibition attenuates ID1 expression in CD44-high glioma-initiating cells. *Neuro Oncol*. 2013; 15:1353–1365. [PubMed: 23877317]
21. Griffin M, Casadio R, Bergamini CM. Transglutaminases: nature's biological glues. *Biochem J*. 2002; 368:377–396. [PubMed: 12366374]
22. Griffin M, Mongeot A, Collighan R, Saint RE, Jones RA, Coutts IG, et al. Synthesis of potent water-soluble tissue transglutaminase inhibitors. *Bioorg Med Chem Lett*. 2008; 18:5559–5562. [PubMed: 18812257]
23. Gundemir S, Colak G, Tucholski J, Johnson GV. Transglutaminase 2: a molecular Swiss army knife. *Biochim Biophys Acta*. 2012; 1823:406–419. [PubMed: 22015769]
24. Gundemir S, Johnson GV. Intracellular localization and conformational state of transglutaminase 2: implications for cell death. *PLoS One*. 2009; 4:e6123. [PubMed: 19568436]
25. Hanahan D, Weinberg RA. Hallmarks of cancer: the next generation. *Cell*. 2011; 144:646–674. [PubMed: 21376230]
26. Herman JF, Mangala LS, Mehta K. Implications of increased tissue transglutaminase (TG2) expression in drug-resistant breast cancer (MCF-7) cells. *Oncogene*. 2006; 25:3049–3058. [PubMed: 16449978]
27. Jang TH, Lee DS, Choi K, Jeong EM, Kim IG, Kim YW, et al. Crystal structure of transglutaminase 2 with GTP complex and amino acid sequence evidence of evolution of GTP binding site. *PLoS One*. 2014; 9:e107005. [PubMed: 25192068]
28. Jans R, Sturniolo MT, Eckert RL. Localization of the TIG3 transglutaminase interaction domain and demonstration that the amino-terminal region is required for TIG3 function as a keratinocyte differentiation regulator. *J Invest Dermatol*. 2008; 128:517–529. [PubMed: 17762858]
29. Keillor JW, Apperley KY, Akbar A. Inhibitors of tissue transglutaminase. *Trends Pharmacol Sci*. 2015; 36:32–40. [PubMed: 25500711]
30. Keillor JW, Chabot N, Roy I, Mulani A, Leogane O, Pardin C. Irreversible inhibitors of tissue transglutaminase. *Adv Enzymol Relat Areas Mol Biol*. 2011; 78:415–447. [PubMed: 22220480]
31. Keillor JW, Chica RA, Chabot N, Vinci V, Pardin C, Fortin E, et al. The bioorganic chemistry of transglutaminase - from mechanism to inhibition and engineering. *Can J Chem*. 2008; 86:271–276.
32. Keillor JW, Clouthier CM, Apperley KY, Akbar A, Mulani A. Acyl transfer mechanisms of tissue transglutaminase. *Bioorg Chem*. 2014; 57:186–197. [PubMed: 25035302]
33. Kiraly R, Csosz E, Kurtan T, Antus S, Szigeti K, Simon-Vecsei Z, et al. Functional significance of five noncanonical Ca²⁺-binding sites of human transglutaminase 2 characterized by site-directed mutagenesis. *FEBS J*. 2009; 276:7083–7096. [PubMed: 19878304]

34. Kumar A, Gao H, Xu J, Reuben J, Yu D, Mehta K. Evidence that aberrant expression of tissue transglutaminase promotes stem cell characteristics in mammary epithelial cells. *PLoS One*. 2011; 6:e20701. [PubMed: 21687668]
35. Kumar A, Xu J, Brady S, Gao H, Yu D, Reuben J, et al. Tissue transglutaminase promotes drug resistance and invasion by inducing mesenchymal transition in mammary epithelial cells. *PLoS One*. 2010; 5:e13390. [PubMed: 20967228]
36. Kumar A, Xu J, Sung B, Kumar S, Yu D, Aggarwal BB, et al. Evidence that GTP-binding domain but not catalytic domain of transglutaminase 2 is essential for epithelial-to-mesenchymal transition in mammary epithelial cells. *Breast Cancer Res*. 2012; 14:R4. [PubMed: 22225906]
37. Lakowicz JR, Szmajdzinski H, Nowaczyk K, Berndt KW, Johnson M. Fluorescence lifetime imaging. *Anal Biochem*. 1992; 202:316–330. [PubMed: 1519759]
38. Lakowicz JR, Szmajdzinski H, Nowaczyk K, Johnson ML. Fluorescence lifetime imaging of free and protein-bound NADH. *Proc Natl Acad Sci U S A*. 1992; 89:1271–1275. [PubMed: 1741380]
39. Liu S, Cerione RA, Clardy J. Structural basis for the guanine nucleotide-binding activity of tissue transglutaminase and its regulation of transamidation activity. *Proc Natl Acad Sci U S A*. 2002; 99:2743–2747. [PubMed: 11867708]
40. Mehta K. Biological and therapeutic significance of tissue transglutaminase in pancreatic cancer. *Amino Acids*. 2009; 36:709–716. [PubMed: 18594944]
41. Nakaoka H, Perez DM, Baek KJ, Das T, Husain A, Misono K, et al. Gh: a GTP-binding protein with transglutaminase activity and receptor signaling function. *Science*. 1994; 264:1593–1596. [PubMed: 7911253]
42. Oliverio S, Amendola A, Di Sano F, Farrace MG, Fesus L, Nemes Z, et al. Tissue transglutaminase-dependent posttranslational modification of the retinoblastoma gene product in promonocytic cells undergoing apoptosis. *Mol Cell Biol*. 1997; 17:6040–6048. [PubMed: 9315663]
43. Pardin C, Roy I, Chica RA, Bonneil E, Thibault P, Lubell WD, et al. Photolabeling of tissue transglutaminase reveals the binding mode of potent cinnamoyl inhibitors. *Biochemistry*. 2009; 48:3346–3353. [PubMed: 19271761]
44. Pardin C, Roy I, Lubell WD, Keillor JW. Reversible and competitive cinnamoyl triazole inhibitors of tissue transglutaminase. *Chem Biol Drug Des*. 2008; 72:189–196. [PubMed: 18715232]
45. Pavlyukov MS, Antipova NV, Balashova MV, Shakhparonov MI. Detection of Transglutaminase 2 conformational changes in living cell. *Biochem Biophys Res Commun*. 2012; 421:773–779. [PubMed: 22548802]
46. Pinkas DM, Strop P, Brunger AT, Khosla C. Transglutaminase 2 undergoes a large conformational change upon activation. *PLoS Biol*. 2007; 5:e327. [PubMed: 18092889]
47. Prime ME, Andersen OA, Barker JJ, Brooks MA, Cheng RK, Toogood-Johnson I, et al. Discovery and structure-activity relationship of potent and selective covalent inhibitors of transglutaminase 2 for Huntington's disease. *J Med Chem*. 2012; 55:1021–1046. [PubMed: 22224594]
48. Rizzo MA, Springer G, Segawa K, Zipfel WR, Piston DW. Optimization of pairings and detection conditions for measurement of FRET between cyan and yellow fluorescent proteins. *Microsc Microanal*. 2006; 12:238–254. [PubMed: 17481360]
49. Rizzo MA, Springer GH, Granada B, Piston DW. An improved cyan fluorescent protein variant useful for FRET. *Nat Biotechnol*. 2004; 22:445–449. [PubMed: 14990965]
50. Siegel M, Khosla C. Transglutaminase 2 inhibitors and their therapeutic role in disease states. *Pharmacol Ther*. 2007; 115:232–245. [PubMed: 17582505]
51. Stamnaes J, Pinkas DM, Fleckenstein B, Khosla C, Sollid LM. Redox regulation of transglutaminase 2 activity. *J Biol Chem*. 2010; 285:25402–25409. [PubMed: 20547769]
52. Sturniolo MT, Chandraratna RA, Eckert RL. A novel transglutaminase activator forms a complex with type 1 transglutaminase. *Oncogene*. 2005; 24:2963–2972. [PubMed: 15846304]
53. Sturniolo MT, Dashti SR, Deucher A, Rorke EA, Broome AM, Chandraratna RA, et al. A novel tumor suppressor protein promotes keratinocyte terminal differentiation via activation of type I transglutaminase. *J Biol Chem*. 2003; 278:48066–48073. [PubMed: 12928434]
54. Wallrabe H, Periasamy A. Imaging protein molecules using FRET and FLIM microscopy. *Curr Opin Biotechnol*. 2005; 16:19–27. [PubMed: 15722011]

55. Yuan L, Siegel M, Choi K, Khosla C, Miller CR, Jackson EN, et al. Transglutaminase 2 inhibitor, KCC009, disrupts fibronectin assembly in the extracellular matrix and sensitizes orthotopic glioblastomas to chemotherapy. *Oncogene*. 2007; 26:2563–2573. [PubMed: 17099729]

Author Manuscript

Author Manuscript

Author Manuscript

Author Manuscript

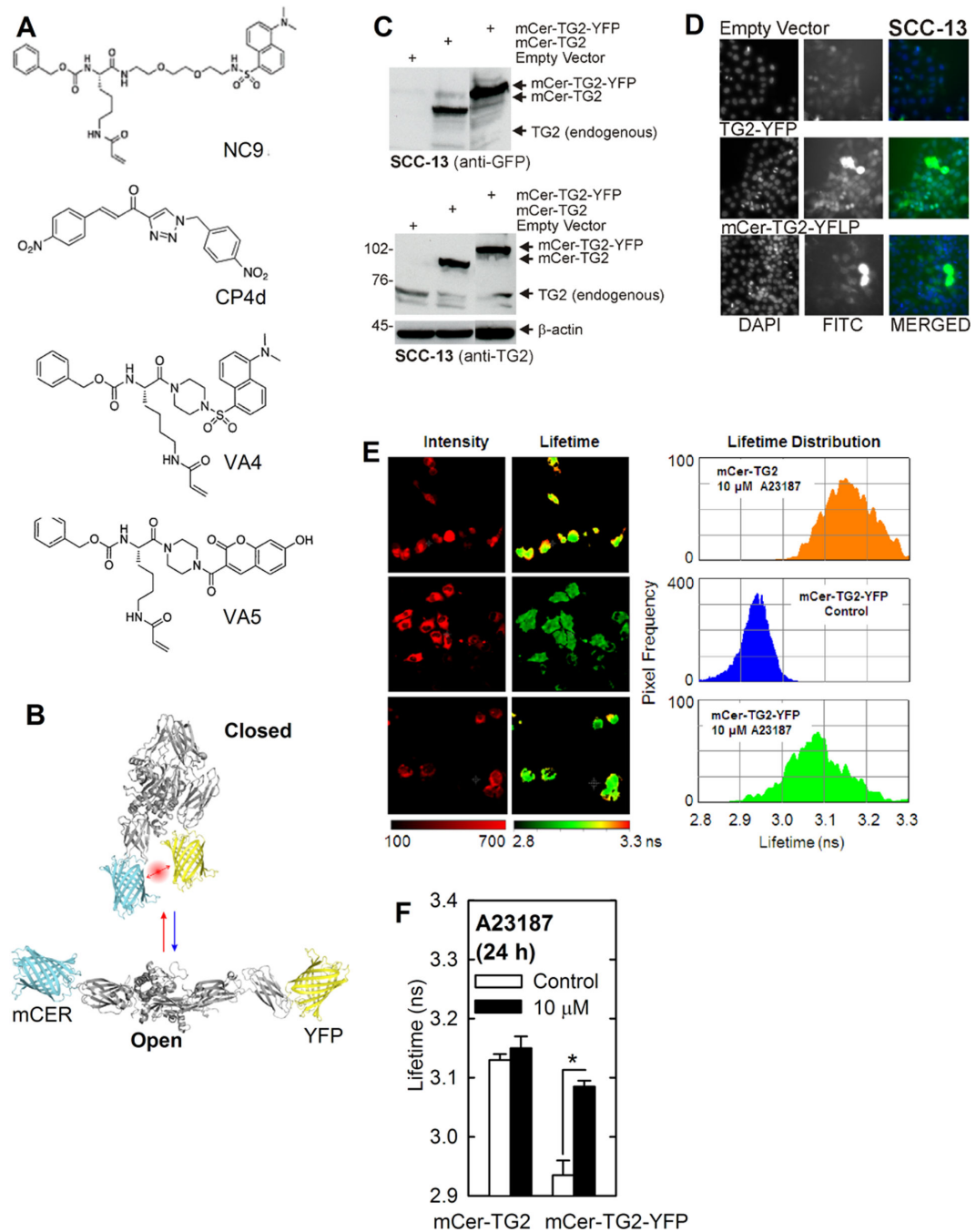


Fig. 1. Calcium regulation of TG2 conformation is detected by FRET/FLIM microscopy
A Structures of TG2 transamidase site-specific acyl-donor substrate competitive (CP4d) and irreversible (NC9, VA4, VA5) inhibitors. **B** Schematic showing closed and extended TG2 conformations and the position of the mCer (donor) and YAP (acceptor) fluorophores. When TG2 is in the closed/folded conformation, the mCer/YFP fluorophores are closely juxtaposed, resulting in efficient energy transfer. In the TG2 open/extended conformation, separation of the fluorophores results in reduced energy transfer efficiency. **C/D** mCer-TG2 and mCer-TG2-YFP are expressed in SCC-13 cells. Cells were electroporated with 3 μg of

each expression plasmid and after 48 h cell extracts were prepared for anti-YFP immunoblot and cells were fixed for anti-YFP cell staining. Note that anti-YFP detects both mCer and YFP. **E** FLIM images of SCC-13 cell electroporated with mCer-TG2 or mCer-TG2-YFP and then treated for 24 h with 10 μ M calcium ionophore (A23187). The left panel show mCer donor intensity and the right panel is fluorescent lifetime for a representative experiment. The histogram plot shows the distribution of lifetimes measured in the assayed cells. **F** The average lifetime in nanoseconds was determined for mCer-TG2 or mCer-TG2-YFP expressing cells treated for 24 h with 0 or 10 μ M A23187. Differences were determined using the students t-test in this and other experiments. The values are mean \pm SEM, n = 6 (p < 0.001).

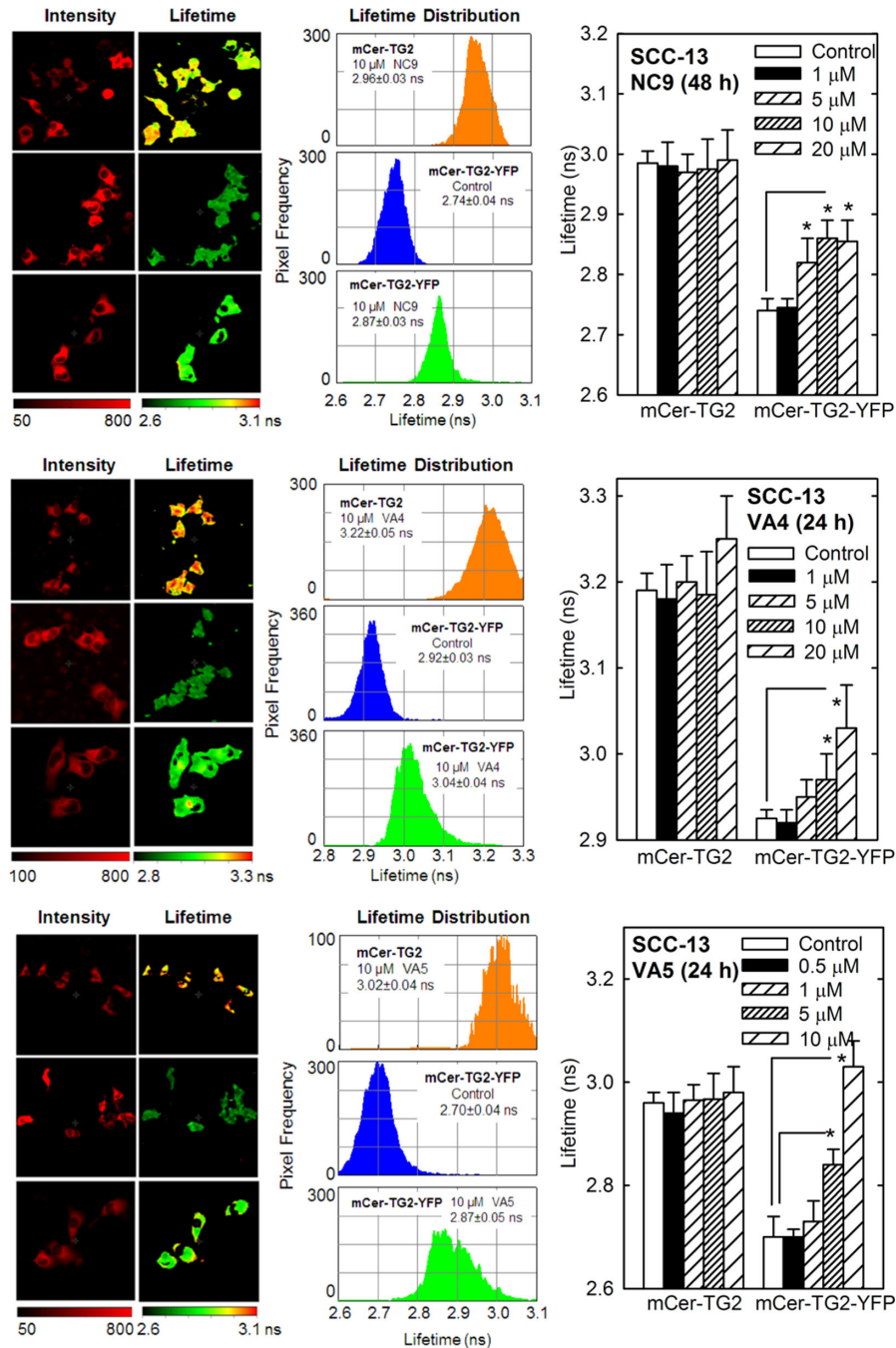


Fig. 2. Irreversible TG2 transamidase site-selective inhibitors shift TG2 from a closed to open conformation

SCC-13 were electroporated with 3 μ g of mCer-TG2 or mCer-TG2-YFP and then incubated with 0 – 20 μ M of NC9, VA4 or VA5 (irreversible TG2 inhibitors) for 24 or 48 h prior to microscopic determination of fluorescence lifetime. mCer donor probe intensity and lifetime images (left) and lifetime distribution histograms (middle) are shown. The plots (right) show the mean lifetime \pm SEM, n = 6 (p < 0.001) for mCer-TG2 and mCer-TG2-YFP expressing cells.

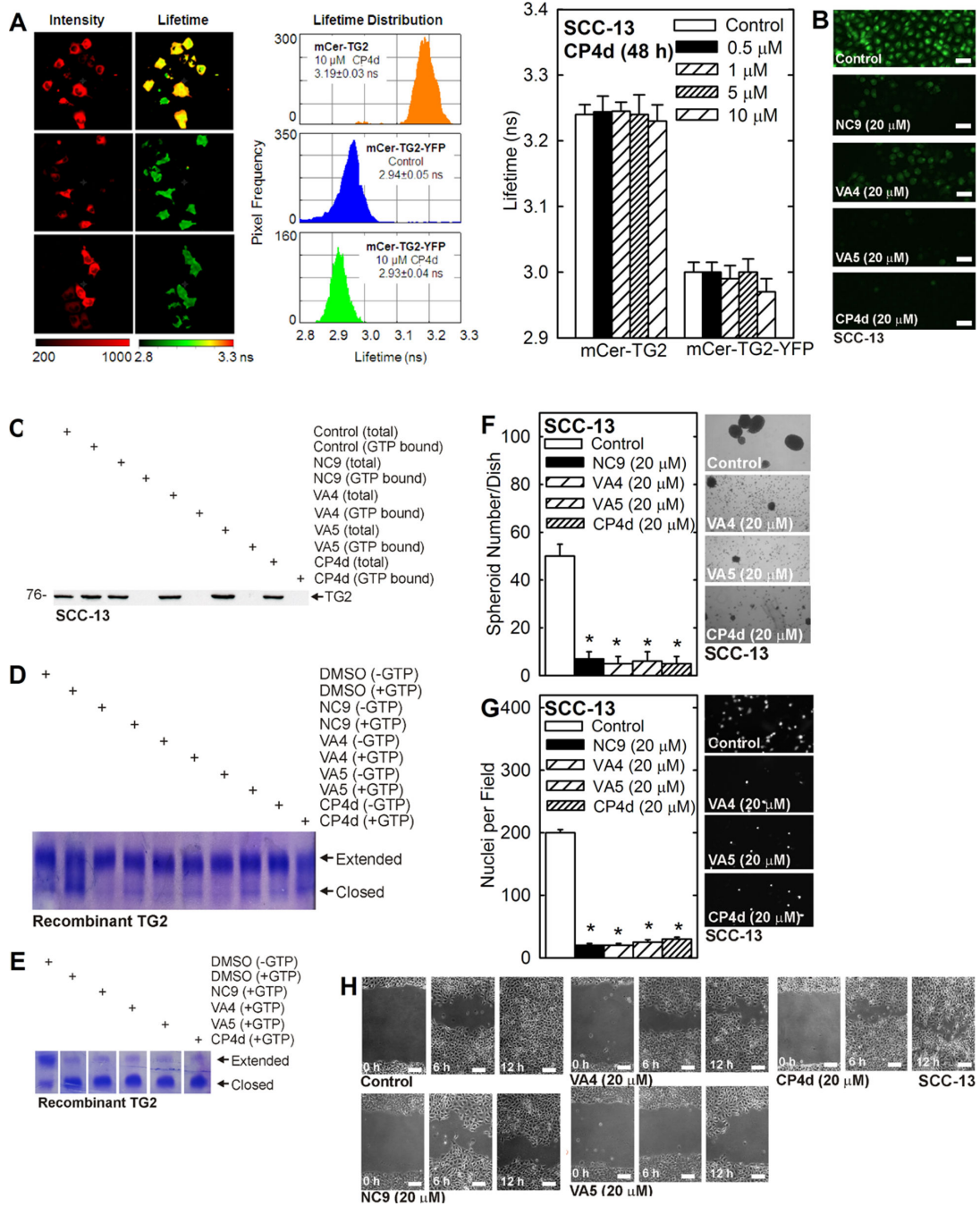


Fig. 3. Impact of CP4d on TG2 structure, and impact of inhibitors on TG2 transamidase/GTP binding activity and biological responses

A CP4d impact on TG2 structure. SCC-13 cells were electroporated 3 μ g of with mCer-TG2 or mCer-TG2-YFP and then incubated for 48 h with 0 – 10 μ M CP4d. Fluorescent intensity and distributions are shown on the left and middle panels. The right panel is a plot showing the average lifetime \pm SEM, n = 4 (p < 0.001). **B** Inhibitor treatment suppresses TG2 transamidase activity. SCC-13 cells were pre-loaded with fluorescein cadaverine (FC) and then challenged with calcium ionophore to increase intracellular calcium and TG2

transamidase activity. The images, which are representative of three separate experiments, show that the inhibitors reduce TG2 transamidase activity as measured by reduced FC crosslinking. **C** Transamidase inhibitors reduce GTP binding to endogenous TG2. SCC-13 cells were incubated for 48 h with the indicated inhibitor and extracts were prepared and incubated with GTP-agarose beads. The beads were then washed, boiled in Laemmli buffer and electrophoresed for immunoblot detection of TG2. Cell equivalent amounts of total extract and pull-down samples were electrophoresed in parallel to facilitate comparison of TG2 bound versus total. Similar results were observed in each of three experiments. **D** Evidence for a direct impact of inhibitors on TG2 structure. Recombinant TG2 was pre-incubated for 1 h with the indicated inhibitor and then challenged with 0 or 500 μ M GTP prior to native gel electrophoresis and coomassie staining. The arrows show migration of the closed and extended forms of TG2. Based on averages from three experiments, the percent TG2 in the closed conformation was as follows: $10 \pm 5\%$ for DMSO(-GTP), $45 \pm 6\%$ for DMSO(+GTP), $2 \pm 0.5\%$ for NC9, AV4 and AV5 (- and + GTP groups), and $2.5 \pm 2\%$ (-GTP) and $10 \pm 2.5\%$ (+GTP) for CP4d. **E** Recombinant TG2 was treated by simultaneous addition of the indicated inhibitor and 500 μ M GTP prior to native gel electrophoresis and coomassie staining. Migration of the closed and extended form is shown. Based on averages from three experiments, the percent TG2 in the closed conformation was as follows: $8 \pm 3\%$ for DMSO(-GTP), $90 \pm 6\%$ for DMSO(+GTP), $2 \pm 0.5\%$ for NC9, AV4, AV5 and CP4d. **F** TG2 inhibitors suppress cancer stem cell survival. SCC-13 cells (20,000 cells) were plated in spheroid growth conditions and permitted to form spheroids for 8 d (2, 18, 19). They were then treated for 48 h with 0 or 20 μ M of the indicated inhibitor and surviving spheroids were counted. The values are mean \pm SEM, $n = 6$ ($p < 0.001$). **G** TG2 inhibitors reduce SCC-13 cell matrigel invasion. SCC-13 cells were plated on a matrigel-coated membrane in the presence of 0 or 20 μ M of the indicated inhibitor and after 24 h the cells migrating to the internal side of the membrane were counted. The values are mean \pm SEM, $n = 6$ ($p < 0.001$). **H** Inhibitors reduce SCC-13 cell migration. Confluent cultures were scratched to generate a wound and closure of this wound was monitored from 0 – 12 h.

inhibitor and extracts were prepared and incubated with GTP-agarose beads to measure TG2 binding to GTP-agarose. The beads were then washed, boiled in Laemmli buffer and electrophoresed for immunoblot detection of TG2. Cell equivalent quantities of total and bound samples were electrophoresed to facilitate comparison of GTP bound versus total. Similar results were observed in each of three experiments. **D/E** Inhibitors suppress HaCaT cell spheroid formation and matrigel invasion. Experiments were performed as described in Fig. 3F/G. The values are mean \pm SEM, n = 4 (p < 0.001). **F/G/H** TG2 is required for NC9 action. SCC-13 TG2 knockout cells, and cells expressing wild-type and reduced TG2 levels, were produced using shRNA-mediated knockdown or CRISPR knockout. TG2 level was monitored by immunoblot and ability of the cells to invade a matrigel layer was assessed as previously described (2, 18). This assay measures the ability of cell to pass through a layer of collagen matrix and is a measure of in vivo invasive/metastatic potential (2). The values are mean \pm SEM, n = 5 (p < 0.001). The reduced invasion observed in TG2-KOc12 cells does not represent a basal migration rate. Migration can be further suppressed by treatment with agents that target proteins other than TG2 (not shown), but cannot be further suppressed by NC9. **I** Structural analysis of GDP binding at nucleotide binding site in TG2 closed and open conformations (details in text).